




Finite Element Analysis of Cannulated Screws as Prophylactic Intervention of Hip Fractures

Geriatric Orthopaedic Surgery
& Rehabilitation
Volume 12: 1–8
© The Author(s) 2021
Article reuse guidelines:
sagepub.com/journals-permissions
DOI: 10.1177/21514593211055890
journals.sagepub.com/home/gos


Brian Rhee¹ , Steven M. Tommasini, PhD¹, Kenneth Milligan, MD¹, Julia Moulton², Michael Leslie, DO, FAOA¹, and Daniel H. Wiznia, MD¹ 

Abstract

Introduction: The frequency of hip fractures, a major cause of morbidity and mortality for geriatric patients, is expected to increase exponentially in the next few decades. The aim of this study is to assess the ability of stainless-steel cannulated screws to reduce the risk of a femoral neck fracture, if placed prophylactically prior to a fall. **Materials and Methods:** We created finite element models from computed tomography (CT) scan-based 3D models of a geriatric patient through 3D-image processing and model generation software. We used linear finite element simulations to analyze the effect of cannulated screws in the proximal femur in single-leg stance and lateral fall, which were processed for peak von Mises stresses and element failure. **Findings:** Prophylactically placed cannulated screws significantly reduced failure in an osteoporotic proximal femur undergoing lateral fall. Three implanted screws in an inverted triangle formation decreased proximal femoral trabecular failure by 21% and cortical failure by 5%. This reduction in failure was achieved with a 55% decrease in femoral neck failure and 14% in lateral cortex failure. **Conclusion:** Our results indicate that cannulated hip screws in an inverted triangle formation may strengthen an osteoporotic proximal femur in the event of a lateral fall. Mechanical testing on cadaveric or composite models is required to validate these results.

Keywords

geriatric trauma, fragility fracture, finite element analysis, prophylactic treatment, hip fracture, cannulated screw, femoral neck, fracture

Introduction

Hip fractures are a major cause of morbidity and mortality for the geriatric population. 320,000 hip fractures occur in North America every year.¹ Due to the improvement of living standards and health care, this number is expected to increase to 580,000 per year and have an estimated annual health care cost surpassing \$10 billion by 2040.² Furthermore, hip fractures severely impact the quality of life of the elderly and have a high risk of mortality.^{3,4} Studies have shown that 2% to 12% of patients with a hip fracture sustain a contralateral fracture in the subsequent 5 years.⁵

In order to cater to the aging population and rising prevalence of osteoporosis, there has been a rapid

development of medication aimed to treat osteoporosis.^{6,7} Studies show that bisphosphonates can result in a 40–50% reduction in femoral neck fractures, but have multiple side effects and require regular doses to maintain their effectiveness.⁸

¹Yale University School of Medicine, New Haven, CT, USA

²Quinnipiac University Frank H. Netter M.D. School of Medicine, North Haven, CT, USA

Corresponding Author:

Daniel Wiznia, Yale University School of Medicine, 47 College Street
New Haven, CT 06510, USA.
Email: Daniel.wiznia@yale.edu



Creative Commons Non Commercial CC BY-NC: This article is distributed under the terms of the Creative Commons Attribution-NonCommercial 4.0 License (<https://creativecommons.org/licenses/by-nc/4.0/>) which permits non-commercial use, reproduction and distribution of the work without further permission provided the original work is attributed as specified on the

SAGE and Open Access pages (<https://us.sagepub.com/en-us/nam/open-access-at-sage>).

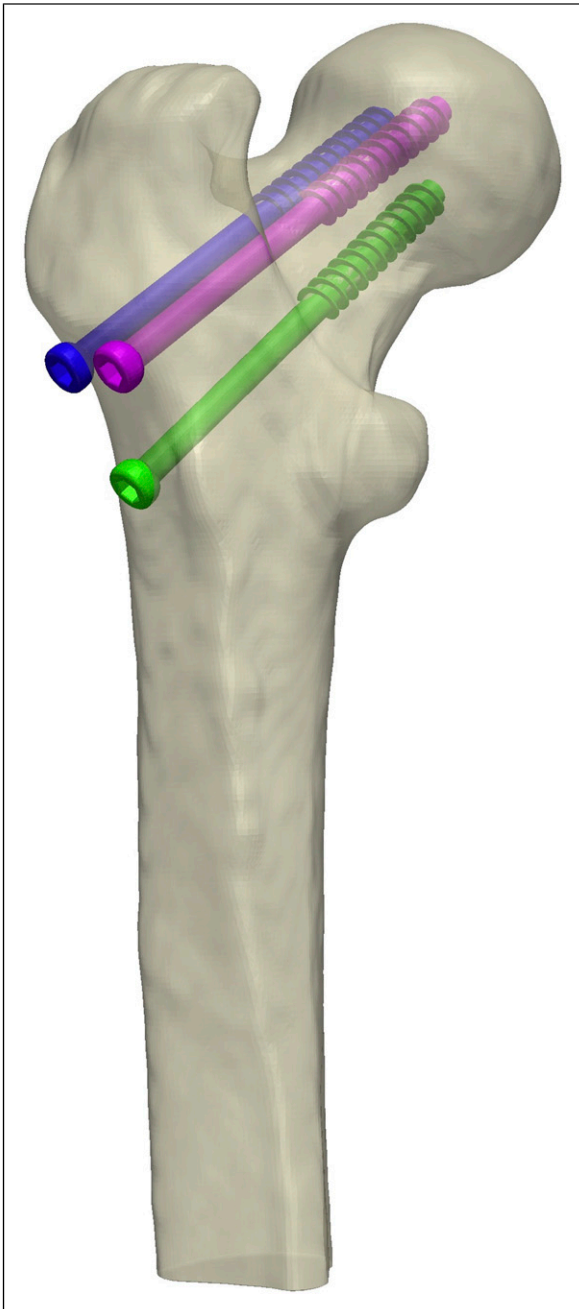


Figure 1. A figure of an implant with three screws in an inverted triangle formation. The control model has no screws. The 1-screw configuration includes the inferior green screw. The 2-screw model incorporates the inferior green and anterior superior magenta screw, and the 3-screw model includes the aforementioned screws and the dark blue posterior superior screw. The 80mm screws were selected to drill into the cortical bone in the femoral head, with the tips less than 1 cm from the subchondral bone medial superior part of the head.

Studies have also investigated whether internal prophylactic augmentation of the proximal femur can be utilized to reinforce the bone and prevent a hip fracture.⁹

Studies have demonstrated that cannulated screws, an inexpensive medical device widely available for managing fractures, may be used to improve the mechanical properties of the femoral neck.¹⁰⁻¹² These studies were limited in several ways. First, the studies utilized polymethyl methacrylate (PMMA) bone cement, which can strengthen the proximal femoral bone in lateral fall, but may cause cell necrosis due to induced pressure of the injection, the exothermic reaction, or toxic unreacted monomers.¹³⁻¹⁵ Furthermore, studies show that augmenting PMMA bone cement in the femoral neck may subsequently result in subtrochanteric fractures, and may introduce significant challenges to a revision surgery as PMMA is biologically inert and permanent, and may interfere with revision instrumentation.¹⁶

It remains unclear if 3 uncemented cannulated screws placed in the configuration of an inverted triangle is a feasible means to prophylactically prevent a contralateral hip fracture. The inverted triangle configuration is known to block the displacement of a femoral neck fracture. This study evaluates through finite element analysis (FEA), an effective method to predict the proximal femur's mechanical properties, to determine whether this configuration of 3 cannulated screws placed prophylactically may strengthen the compressive trabeculae's mechanical properties and lower fracture risk in the femoral neck.¹⁷

Methods

Materials

A 7.3 mm, 32 mm partially threaded cannulated screw with 80 mm length manufactured by DePuy Synthes (reference number 209.900) was modeled in SolidWorks (Dassault Systèmes, Waltham, MA) and exported in STL (Standard Tessellation Language) format. This screw, composed of SS316L stainless steel and designed to manage femoral neck fractures, is available in varying shaft and thread lengths. A set of CT scans of a 68-year-old Caucasian female donor was scanned in air on a Philips Brilliance 64 CT system with a bone mineral reference phantom (Mindways, Austin, TX) at 120 kVp and 200 mA. The scans had an in-plane pixel size of $.6895 \times .6895$ mm with a .9 mm slice thickness and voxel resolution of $512 \times 512 \times 230$. The height and mass of donor were estimated using the femoral characteristics derived from the CT scan.^{18,19}

Model Formation With ScanIP

The CT scans were imported into the ScanIP module in Simpleware (Synopsys Inc, Mountain View, CA). The scans were processed using ScanIP's geometric functions and filters to close holes, fill cavities, remove islands, and smooth the final product. To allow for uniform loading of the femoral

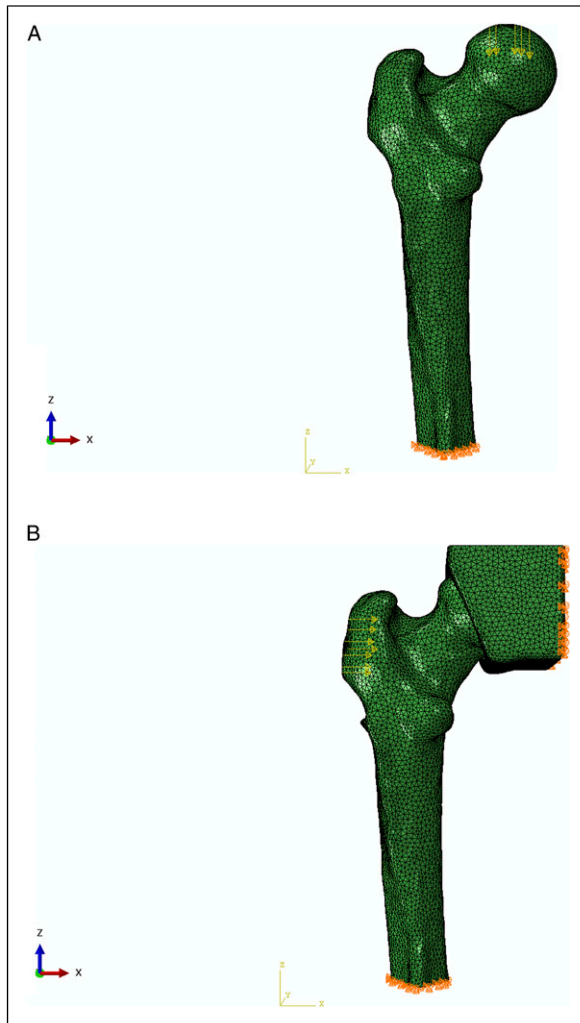


Figure 2. (A) A representation of the weighting simulation, where the femur is constrained on the distal end and a downwards load is placed on the femoral head. (B) A diagram representing the forces that simulate a sideways fall, where constraints are placed on a simulated acetabulum and distal end of the femur.

head, the proximal femur was coupled with a socket mimicking the shape of an acetabulum. In order to analyze femoral failure, the acetabulum was assigned a high Young's modulus (100 GPa) to simulate a stiff material that will not deform under loading. STL files of the cannulated screws were imported as surfaces and positioned using the position and orientation functions of the surface tool feature, where they were then modelled as bonded contacts to the bone. Finally, the surface-to-mask, subtractive Boolean, and recursive gaussian functions were used to remove and smooth bone that would be drilled through to place the guidewires during surgical procedures. The screw positions were confirmed by 2 attending orthopedic surgeons with trauma fellowship training.

Four FE models—a control without a screw, as well as 1-screw, 2-screw, and 3-screw models—were exported with no particular node sets, shells, or boundary layers (Figure 1) in 3

bone qualities—healthy, osteopenic, and osteoporotic—derived from literature.²⁰ The control, 1-screw, 2-screw, and 3-screw models were exported as tetrahedra linear models and have 41 707, 138 297, 226 825, and 318 039 elements, respectively. The QCT density was converted to wet apparent density based on mechanical testing studies, and the Young's Modulus was determined as a function of density (.76, .71, and .63 g/cc average densities for healthy, osteopenic, and osteoporotic bone, respectively).^{21,22} ScanIP defined the femur as 7 discrete materials with ranging Young's moduli and defined cortical bone as any material with a wet apparent density greater than 1 g/cc.²³

Abaqus/CAE Single Leg Stance Simulation

The 4 femur models were exported to Abaqus/CAE (Dassault Systemes) for a standing simulation. As shown in Figure 2A, the distal portion of the femur was constrained and the load was placed on the top of the femoral head to simulate a single-leg stance configuration. The load was estimated as 2.5 times the patient's weight w , as shown in equation (1).²⁴

$$F_{\text{stance}}(N) = 2.5w \quad (1)$$

Abaqus/CAE Lateral Fall Simulation

Subsequently, the femur models were subjected to a fall simulation in Abaqus/CAE. As shown in Figure 2B, a force is loaded onto the greater trochanter region of the femur, which is constrained distally and by the simulated acetabulum proximally to allow for uniform loading across the femoral head. The impact force was determined by the patient's weight w in Newtons and height h in centimeters as shown below^{25,26}

$$F_{\text{fall}}(N) = 8.25 * w \left(\frac{h}{170} \right)^{0.5} \quad (2)$$

The femur models were also subjected to a lateral fall that was tripled in magnitude in order to determine if the cannulated screw implants can mitigate loads of a higher energy sideways fall.

The results from the Abaqus/CAE simulations were exported and then analyzed using in-house MATLAB codes (R2020a, MathWorks, Natick MA). Based on Bessho et al., the ultimate tensile strength (UTS) of each element can be calculated on the ash density ρ (g/cm³), which was obtained from a correlation with the apparent wet density.^{24,27,28} Elements were considered failed when they surpassed their respective UTS.

$$\text{UTS(MPa)} = 137\rho^{1.88} \quad \text{for } \rho < 0.317 \quad (3)$$

Table 1. Single-Leg Stance, Lateral Fall, and Tripled Lateral Fall Simulation Results, Summarizing the Peak Stresses and Volumetric Failure (VFP) for Normal, Osteopenic, and Osteoporotic Conditions. The VFP was Categorized into Trabecular and Cortical Failure in Order to Assess How Each Respective Region was Impacted.

Simulation	Weight						Lateral Fall						Lateral Fall, Tripled					
	Peak Stress (MPa)	Failed Volume (mm ³)	VFP (%)		Peak Stress (MPa)	Failed Volume (mm ³)	Peak Stress (MPa)	Failed Volume (mm ³)	VFP (%)		Peak Stress (MPa)	Failed Volume (mm ³)	VFP (%)		Peak Stress (MPa)	Failed Volume (mm ³)	VFP (%)	
			Trabecular	Cortical					Trabecular	Cortical			Trabecular	Cortical			Trabecular	Cortical
Control, healthy	38.6	.00 × 10 ⁰	.0%	.00%	89.3	1.81 × 10 ⁴	8.3%	.0%	8.33%	272.1	6.60 × 10 ⁴	30.0%	.3%	30.29%				
1 Screw, healthy	39.1	6.16 × 10 ⁰	.0%	.00%	88.5	1.80 × 10 ⁴	8.3%	.0%	8.33%	269.5	6.49 × 10 ⁴	29.7%	.3%	30.02%				
2 Screws, healthy	34.9	2.03 × 10 ¹	0.0%	.01%	179.7	1.61 × 10 ⁴	7.5%	.0%	7.52%	547.4	6.19 × 10 ⁴	28.6%	.2%	28.80%				
3 Screws, healthy	59.7	3.45 × 10 ¹	.0%	.02%	177.6	1.50 × 10 ⁴	7.0%	.0%	7.02%	540.6	5.85 × 10 ⁴	27.2%	.2%	27.43%				
Control, osteopenic	37.9	.00 × 10 ⁰	.0%	.00%	96.7	2.41 × 10 ⁴	11.0%	.1%	11.08%	290.0	7.20 × 10 ⁴	32.7%	.4%	33.04%				
1 Screw, osteopenic	39.9	1.04 × 10 ¹	.0%	.00%	92.7	2.37 × 10 ⁴	10.9%	.1%	10.98%	280.0	7.05 × 10 ⁴	32.3%	.4%	32.65%				
2 Screws, osteopenic	36.2	3.12 × 10 ¹	.0%	.01%	203.4	2.11 × 10 ⁴	9.8%	.1%	9.82%	610.5	6.74 × 10 ⁴	31.1%	.3%	31.37%				
3 Screws, osteopenic	74.2	5.39 × 10 ¹	.0%	.03%	205.9	1.90 × 10 ⁴	8.8%	.0%	8.90%	622.4	6.40 × 10 ⁴	29.7%	.3%	30.02%				
Control, osteoporotic	38.4	2.17 × 10 ¹	.0%	.01%	102.4	3.37 × 10 ⁴	15.4%	.1%	15.47%	311.5	8.28 × 10 ⁴	37.6%	.4%	38.00%				
1 Screw, osteoporotic	43.3	5.90 × 10 ¹	.0%	.03%	90.2	3.44 × 10 ⁴	15.9%	.0%	15.93%	274.4	8.15 × 10 ⁴	37.4%	.3%	37.71%				
2 Screws, osteoporotic	39.9	7.03 × 10 ¹	.0%	.03%	161.8	3.08 × 10 ⁴	14.3%	.1%	14.34%	485.3	7.75 × 10 ⁴	35.8%	.3%	36.08%				
3 Screws, osteoporotic	59.7	1.89 × 10 ²	.1%	.09%	158.0	2.66 × 10 ⁴	12.4%	.1%	12.47%	477.3	7.44 × 10 ⁴	34.6%	.3%	34.88%				

$$\text{UTS(MPa)} = 114\rho^{1.72} \quad \text{for } \rho \geq 0.317 \quad (4)$$

The volumetric percentage of failed elements exceeding the UTS (VFP) was calculated for cortical and trabecular regions of the bone, as each type of bone mechanically supports the femur under different types of loads.²⁹

$$\text{VFP(\%)} = \frac{\text{vol. elements surpassing UTS}}{\text{total volume}} * 100 \quad (5)$$

Results

Fracture Risk and Volumetric Failure Analysis

The single-leg stance results (Table 1) demonstrate that there is a general increase in peak stress in the bone as more screws are added to the model. Peak stresses in the control model remained comparable at an average of 38 MPa across declining bone quality, while the models containing screws experienced varied results. As bone quality deteriorated,

models containing screws experienced a significant increase in volumetric failure. Furthermore, the 2 and 3 screw models experienced a slightly significant increase in volumetric failure ($X^2(1) = 22.1$, $P = .003$).

Lateral fall results (Table 1) demonstrated that models with screws—in particular the 2 screw and 3 screw model—experienced higher peak stress in the bone (average von Mises peak stress of 181 MPa) in comparison to the control model, but had decreased failed volume and VFP (averaged $2.14 \times 10^4 \text{ mm}^3$, $X^2(1) = 47.2$, $P < .001$). All models experienced an increase in volumetric failure as the bone quality decreased, and experienced the majority of the failure in the trabecular region of the femur. These trends were seen in the lateral fall simulations with a tripled magnitude ($X^2(1) = 5.2$, $P = .513$).

Cortical and Trabecular Element Failure

Abaqus/CAE screenshots of the osteoporotic lateral fall simulations (Figure 3) indicate that the interface between

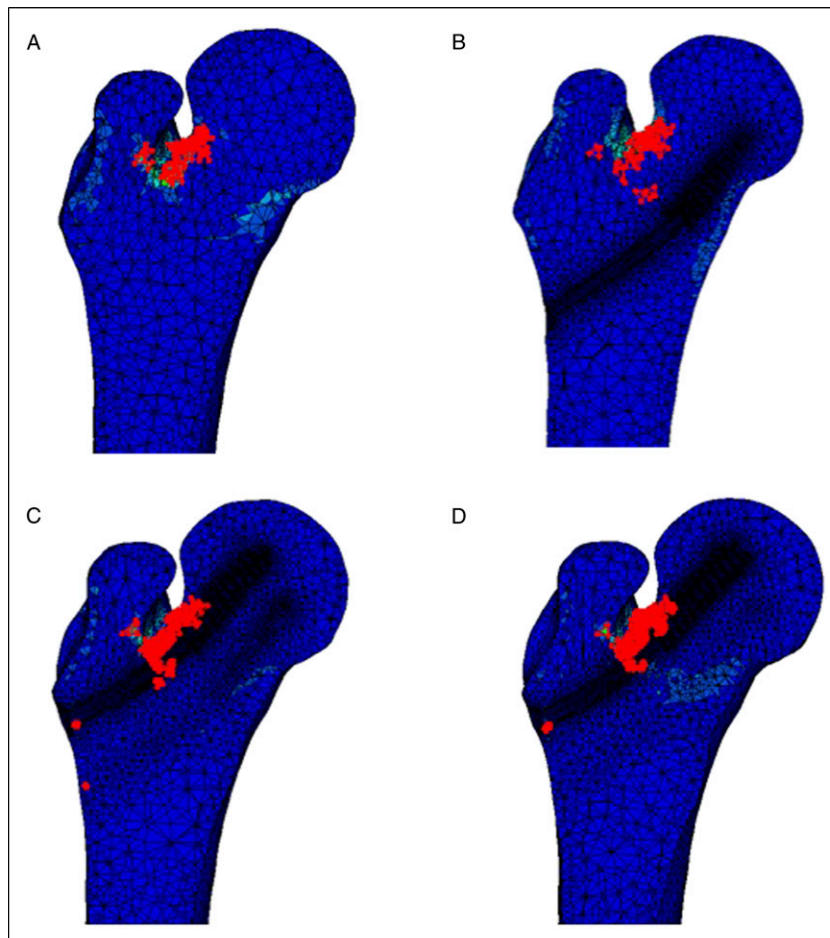


Figure 3. Location of failed cortical elements (red) within an osteoporotic proximal femur with (A) no implants, (B), 1, (C) 2, or (D) 3 cannulated screws implanted. Volumetric cortical element failure was smaller in the models containing screws in comparison to the control model.

Table 2. Failed Volume in an Osteoporotic Femur From a Lateral Fall. Having 2 or 3 Screws Reduces Both Trabecular and Cortical Failure.

Simulation Name	Failed Volume (mm ³)		% Reduction	
	Trabecular	Cortical	Trabecular	Cortical
Control, Osteoporotic	33595.2	116.6	-	-
1 Screw, Osteoporotic	34317.9	87.3	-2.15%	25.16%
2 Screws, Osteoporotic	30692.0	114.7	8.64%	1.64
3 Screws, Osteoporotic	26486.3	110.2	21.16%	5.52%

Table 3. Lateral Fall Simulation Results of the Femoral Neck and Lateral Cortex. The Peak Stresses for the Overall Models Were Located in the Femoral Neck. The 1 Screw Models Peak Stresses Were Located on the Distal Side of the Femoral Neck. Lateral Cortex and Femoral Neck Volumetric Failure Decrease in the 2 and 3 Screw Models.

Simulation Name	Femoral Neck			Lateral Cortex		
	Peak Stress (MPa)	Failed Volume (mm ³)	% Reduction	Peak Stress (MPa)	Failed Volume (mm ³)	% Reduction
Control, healthy	89.3	4.91 × 10 ³	-	68.7	8.13 × 10 ³	-
1 Screw, healthy	75.9	4.75 × 10 ³	-3%	58.1	7.92 × 10 ³	-3%
2 Screws, healthy	179.7	2.83 × 10 ³	-43%	84.2	7.88 × 10 ³	-3%
3 Screws, healthy	177.6	1.84 × 10 ³	-63%	53.6	7.43 × 10 ³	-9%
Control, osteopenic	96.7	6.95 × 10 ³	-	76.7	1.00 × 10 ⁴	-
1 Screw, osteopenic	80.3	6.70 × 10 ³	-4%	61.7	9.60 × 10 ³	-4%
2 Screws, osteopenic	203.4	4.24 × 10 ³	-39%	92.4	9.29 × 10 ³	-7%
3 Screws, osteopenic	205.9	2.64 × 10 ³	-62%	58.1	8.74 × 10 ³	-13%
Control, osteoporotic	102.4	9.67 × 10 ³	-	86.1	1.25 × 10 ⁴	-
1 Screw, osteoporotic	90.2	9.92 × 10 ³	3%	75.2	1.13 × 10 ⁴	-10%
2 Screws, osteoporotic	161.8	7.13 × 10 ³	-26%	80.1	1.16 × 10 ⁴	-7%
3 Screws, osteoporotic	158.0	4.38 × 10 ³	-55%	72.1	1.08 × 10 ⁴	-14%

the screw heads and lateral cortex of the femur experienced additional stress in the 2 and 3 screw models, but did not substantially increase the amount of cortical failure. Volumetric analysis (Table 2) demonstrates that 2 or 3 screws reduce the failure in osteoporotic cortical and trabecular bone ($X^2(1) = 12.9, P = .005$). Furthermore, isolated analyses of the femoral neck and lateral cortex (Table 3) demonstrate that the failure is not being transferred from the femoral neck to the lateral cortex. The 3 screw models exhibit this behavior the most, reducing femoral neck and lateral cortex failure by approximately 60% and 12%, respectively, with respect to the control model.

Discussion

Fragility fractures are a rising cause for geriatric morbidity and mortality. While pharmacologic treatments reduce fracture risk, they cannot be implemented for all patients. Ongoing research has been assessing whether orthopedic implants can be used as prophylactic treatments. This study

utilized linear FEA to evaluate if proximal fracture risk can be mitigated with an inverted triangle configuration of uncemented cannulated screws. Our findings suggest that 2 or 3 cannulated screws in this formation will strengthen the proximal femur during lateral fall without translating stress to the femoral neck or lateral cortex. These screws may increase stress experienced on the proximal femur during stance but will not increase to a level of failure. It is unclear to what degree the proximal femur must be strengthened to prevent fractures caused by lateral fall or stance. Our results highlight how cannulated screws can strengthen the proximal femur without inducing significant stress during stance. As such, biomechanical studies using composite bones are currently ongoing to confirm these results and validate whether prophylactic intervention of cannulated screws will prevent femoral fractures.

There are a few limitations that should be considered with this study. This analysis simplifies proximal femur loading, the degrees of freedom in femoral movement, and the material properties of bone. Furthermore, our non-

validated linear simulations do not account for localized failure and do not assess the microarchitecture and micro-mechanical properties of bone may result in inaccurate predictions of bone failure.

During a single-leg stance, screws may cause an increase in peak stress in the bone. This is most apparent in the osteopenic bone model, where the peak stresses located at the screw head and lateral cortex interface doubled with respect to the control model, but did not surpass the ultimate strength of the femur. Additionally, the models containing screws had higher failed volumes than the control model, which was located on the lateral cortex interface and some threads of the screws. This suggests that during stance, screws act as a stress riser by translating the stress experienced on the femoral head to the lateral cortex. Furthermore, screws may cause stress concentrations as the screw threads compress the inferior femoral neck during this type of loading.

Lateral fall simulations suggest that cannulated screws can be used to provide immediate strength of the femoral neck (Table 1). Having 1 screw in the femur model had a marginal impact in reducing fracture risk, with a minimal improvement in trabecular failure and detrimental effects on cortical bone (Table 2). However, the 2 and 3 screw models saw a substantial improvement of femoral neck fracture risk. Depending on the bone density, the volumetric failure decrease ranged from 11% to 21% with respect to the control model. Similar trends were found in the lateral fall simulation with a high energy triple load (Table 1), where volumetric failure reduction varied from 6% to 11%. The models containing screws typically exhibited higher peak stresses regardless of bone quality. Although having 1 screw did not change failure with respect to the control model, 2 or more screws resulted in a significant reduction in fracture risk indicated by a reduction in the failed volume analyses.

In order to confirm that the fracture risk was not being transferred to the lateral cortex, we conducted isolated analyses of the femoral neck and lateral cortex regions. Results from the lateral cortex analysis (Table 3) demonstrated that models containing screws experienced a decrease in volumetric failure regardless of the bone quality despite having higher peak stresses in comparison to the control model. Furthermore, failed volumes from the femoral neck results are significantly lower in the 2 and 3 screw models compared to the control model. As peak stresses from the overall analysis are found in the femoral neck region, these results suggest that the primary failure will still occur in the femoral neck region, without shifting the stress and failure site to the lateral cortex region.

Conclusion

This study assesses the performance of cannulated hip screws as a prophylactic intervention of proximal hip fracture due to a lateral fall. The results suggest that implanting 2 or 3 screws in an inverted triangle formation strengthen the femoral neck during a lateral fall without translating the failure to another region. Further biomechanical testing is required to confirm these results before clinical use is considered.

Acknowledgements

The study gratefully acknowledges Dr R. Dana Carpenter, Associate Professor at University of Colorado Denver, for providing the initial calibrated Simpleware ScanIP femur model.

Declaration of conflicting interests

The author(s) declared no potential conflicts of interest with respect to the research, authorship, and/or publication of this article.

Funding

This work was supported by CTSA Grant UL1 TR001863 from the National Center for Advancing Translational Science (NCATS), a component of the National Institutes of Health (NIH), and NIH Roadmap for Medical Research. Its contents are solely the responsibility of the authors and do not necessarily represent the official view of NIH.

Disclosures

Brian Rhee (N), Steven M. Tommasini (N), Kenneth Milligan (N), Julia Moulton (N), Michael Leslie (N), Daniel Wiznia (3B-Intellijoint Surgical)

ORCID iDs

Brian Rhee  <https://orcid.org/0000-0002-3264-7461>

Daniel H. Wiznia  <https://orcid.org/0000-0003-3987-0364>

References

1. The National Institute of Health and Care Excellence. *NICE Clinical Guideline 124: The Management of Hip Fracture in Adults*. London: Royal College of Physicians; 2011.
2. Schemitsch E, Bhandari M. Femoral neck fractures: Controversies and evidence. *J Orthop Trauma*. 2009;23(6):385.
3. Mundi S, Pindiprolu B, Simunovic N, Bhandari M. Similar mortality rates in hip fracture patients over the past 31 years: A systematic review of RCTs. *Acta Orthop*. 2014;85(1):54-59.
4. Parkkari J, Kannus P, Palvanen M, Natri A, Vainio J, Aho H, et al. Majority of hip fractures occur as a result of a fall and impact on the greater trochanter of the femur: A prospective

- controlled hip fracture study with 206 consecutive patients. *Calcif Tissue Int.* 1999;65(3):183-187.
5. Hughes JD, Bartley JH, Brennan KL, Maldonado YM, Brennan ML, Chaput CD. Rate of contralateral hip fracture after dynamic hip screw vs intramedullary nail for treatment of pertrochanteric hip fractures. *Proc (Bayl Univ Med Cent)*. 2017;30(3):268-272.
 6. Appelman-Dijkstra NM, Papapoulos SE. Modulating bone resorption and bone formation in opposite directions in the treatment of postmenopausal osteoporosis. *Drugs*. 2015;75:1049-1058.
 7. Zhou S, Huang G, Chen G. Synthesis and biological activities of drugs for the treatment of osteoporosis. *Eur J Med Chem*. 2020;197:112313.
 8. Srivastava M, Deal C. Osteoporosis in elderly: Prevention and treatment. *Clin Geriatr Med*. 2002;18(3):529-555.
 9. Varga P, Hofmann-Fliri L, Blauth M, Windolf M. Prophylactic augmentation of the osteoporotic proximal femur—mission impossible? *Bonekey Rep*. 2016 7;5:854.
 10. Khoo C, Haseeb A, Ajit Singh V. Cannulated Screw fixation for femoral neck fractures: A 5-year experience in a single institution. *Malays Orthop J*. 2014;8(2):14-21.
 11. Zwicky L. *Prophylactic Stabilization of Osteoporotic Femora for Fracture Prevention (In German)*. [MSc thesis]. Switzerland: ETH Zürich, Davos and Zurich; 2008.
 12. *Laboratory for Bone Biomechanics*. Master's Thesis. ETH Zurich. Zürich, Switzerland.
 13. Feng H, Feng J, Li Z, Feng Q, Zhang Q, Qin D, et al. Percutaneous femoroplasty for the treatment of proximal femoral metastases. *Eur J Surg Oncol*. 2014;40:402-405.
 14. Varga P, Inzana JA, Schwiedrzik J, Zysset PK, Gueorguiev B, Blauth M, et al. New approaches for cement-based prophylactic augmentation of the osteoporotic proximal femur provide enhanced reinforcement as predicted by nonlinear finite element simulations. *Clin Biomech (Bristol, Avon)*. 2017;44:7-13.
 15. Heini PF, Franz T, Fankhauser C, Gasser B, Ganz R. Femoroplasty-augmentation of mechanical properties in the osteoporotic proximal femur: A biomechanical investigation of PMMA reinforcement in cadaver bones. *Clin Biomech*. 2004;19:506-512.
 16. Beckmann J, Ferguson SJ, Gebauer M, Luering C, Gasser B, Heini P. Femoroplasty-augmentation of the proximal femur with a composite bone cement—feasibility, biomechanical properties and osteosynthesis potential. *Med Eng Phys*. 2007;29:755-764.
 17. Varga P, Schwiedrzik J, Zysset PK, Fliri-Hofmann L, Widmer D, Gueorguiev B, et al. Nonlinear quasi-static finite element simulations predict in vitro strength of human proximal femora assessed in a dynamic sideways fall setup. *J Mech Behav Biomed Mater*. 2016;57:116-127.
 18. Pomeroy E, Mushrif-Tripathy V, Kulkarni B, Kinra S, Stock JT, Cole TJ, et al. Estimating body mass and composition from proximal femur dimensions using dual energy x-ray absorptiometry. *Archaeol Anthropol Sci*. 2019;11(5):2167-2179.
 19. Zech WD, Näf M, Siegmund F, Jackowski C, Löscher S. Body height estimation from post-mortem CT femoral F1 measurements in a contemporary Swiss population. *Leg Med (Tokyo)*. 2016;19:61-66.
 20. Helgason B, Perilli E, Schileo S, Taddei F, Brynjólfsson S, Viceconti M. Mathematical relationships between bone density and mechanical properties: A literature review. *Clin BioMech*. 2008;23(2):135-146.
 21. Lotz JC, Gerhart TN, Hayes WC. Mechanical properties of trabecular bone from the proximal femur: A quantitative CT study. *J Comput Assist Tomogr*. 1990;14(1):107-114.
 22. Morgan EF, Bayraktar HH, Keaveny TM. Trabecular bone modulus-density relationships depend on anatomic site. *J Biomech*. 2003;36(7):897-904.
 23. Reilly DT, Burstein AH. The elastic and ultimate properties of compact bone tissue. *J Biomech*. 1975;8(6):393-405.
 24. Bessho M, Ohnishi I, Matsuyama J, Matsumoto T, Imai K, Nakamura K. Prediction of strength and strain of the proximal femur by a CT-based finite element method. *J Biomech*. 2007;40(8):1745-1753.
 25. Yoshikawa T, Turner CH, Peacock M, Slemenda CW, Weaver CM, Teegarden D, et al. Geometric structure of the femoral-neck measured using dual-energy X-ray absorptiometry. *J Bone Miner Res*. 1994;9:1053-1064.
 26. Miura M, Nakamura J, Matsuura Y, Wako Y, Suzuki T, Hagiwara S, et al. Prediction of fracture load and stiffness of the proximal femur by CT-based specimen specific finite element analysis: Cadaveric validation study. *BMC Musculoskelet Disord*. 2017;18:536.
 27. Keyak JH, Lee IY, Skinner HB. Correlations between orthogonal mechanical properties and density of trabecular bone: Use of different densitometric measures. *J Biomed Mater Res*. 1994 Nov;28(11):1329-1336.
 28. Pétursson Þ, Edmunds KJ, Gíslason MK, Magnússon B, Magnúsdóttir G, Halldórsson G, et al. Bone mineral density and fracture risk assessment to optimize prosthesis selection in total hip replacement. *Comput Math Methods Med*. 2015; 2015:162481.
 29. Ott S M. Cortical or trabecular bone: What's the difference? *Am J Nephrol*. 2018;47:373-375.